2003-10-15

# Allowed mesoscopic point group symmetries in domain average engineering of perovskite ferroelectric crystals

Dorian M. Hatch
hatchd@byu.edu

H. T. Stokes

W. Cao

# Allowed mesoscopic point group symmetries in domain average engineering of perovskite ferroelectric crystals

D. M. Hatch[a] and H. T. Stokes
*Department of Physics and Astronomy, Brigham Young University, Provo, Utah 84602*

W. Cao[b]
*Department of Physics and Materials Science, City University of Hong Kong, Kowloon, Hong Kong, China*

In multivariant systems, several energetically degenerate low temperature domain states can be produced at the structural phase transition. Coexistence of these domain states can produce mesoscopic structures that possess symmetries distinct from the microscopic single domain crystal symmetry. Such engineered domain structures in certain ferroelectric materials have been proven to give superior piezoelectric properties and extremely soft shear moduli. The objective of this article is to consider the variety of symmetries that can be produced through domain average engineering in proper ferroelectric systems arising from the cubic $Pm3m$ symmetry perovskite structure. © *2003 American Institute of Physics.* [DOI: 10.1063/1.1611634]

## I. INTRODUCTION

Many ferroelectric systems belong to the perovskite family with the high temperature phase having cubic $Pm3m$ symmetry. A ferroelectric phase transition driven by a zone center transverse optical "soft" mode produces a crystal structure with a dipole in each unit cell, reducing the symmetry to one of the polar classes: $1, 2, 3, 4, 6, m, mm2, 3m, 4mm$, and $6mm$. As a consequence, there is more than one low temperature ferroelectric domain state present. A domain refers to a homogeneous crystal region in which all the dipoles are aligned in the same direction. It is a well established fact that the presence of domains can substantially enhance the properties of ferroelectric materials. In a single crystal system, two neighboring domains form a twin structure and there is a spatial transition region between them, which is termed the domain wall, since it usually appears as a planar structure along particular crystallographic orientations. Under an applied external field, the size of ferroelectric domains can either contract or expand in order to lower the total energy of the system, causing the domain walls to move. These domain wall movements and the resulting domain configurations produce the so-called "extrinsic contributions" to the effective material properties in many ceramic ferroelectrics. These extrinsic contributions have been experimentally verified to amount to 60% of the total piezoelectric and dielectric effects in $Pb(Zr,Ti)O_3$ (PZT) ceramics at room temperature. For this reason, researchers have spent extensive effort to find better chemical additives that can enhance the mobility of domain walls. For example, a few percent of La or Nb dopants can produce more than 50% improvement in piezoelectric and dielectric properties in the so called soft PZT ceramics.

Recently, a method has been reported to fabricate desired multidomain single crystals, which can greatly enhance the piezoelectric and the electromechanical coupling coefficients in relaxor-based ferroelectric single crystals of $Pb(Mg_{1/3}Nb_{2/3})O_3$ (PMN–PT) and $Pb(Zn_{1/3}Nb_{2/3})O_3$ (PZN–PT).[1–4] Both solid solution systems have a perovskite structure. Poling along one of the pseudocubic axes, for example [001], in the rhombohedral phase ferroelectric crystals (corresponding to a [111] polarization), creates a multidomain state containing four of the eight possible low temperature variants with the local dipoles oriented randomly along [111], [1̄11], [11̄1] and [111̄] directions with respect to the pseudocubic axes. Such a poled multi-domain system has a piezoelectric coefficient over 2000 pC/N and an electromechanical coupling coefficient $k_{33}$ over 90%,[1,3,4] which is a dream come true for transducer and piezoactuator designers. The complete set of matrix properties have been determined for the PZN–PT and PMN–PT multidomain single crystal based on the pseudotetragonal symmetry, which is substantially different from data of the single domain single crystal and ceramic samples.[3,4] The method used in enhancing the material properties in this case is to manipulate the domain structures instead of the domain wall mobility. Therefore, the configuration and size of the domains will determine the effective symmetry and the average material properties.

It was found that one of the shear moduli in the multi-domain systems is extremely low, which means that the mesoscopic structures can also greatly influence the elastic properties. These results demonstrated that the domain-engineering concept might help us to produce materials with superior properties. In order to take full advantage of this process, one must gain a better understanding of the kinds of effective symmetry that can be produced in each given crystal system. Obviously, the mesoscopic symmetry or symmetry of domain patterns is intrinsically linked to the underlying crystal structure. Here we use group theoretical methods to make a detailed analysis of possible proper ferroelectric

[a]Author to whom correspondence should be addressed; electronic mail: hatchd@byu.edu
[b]Present address: Department of Mathematics, The Pennsylvania State University, University Park, PA 16802.
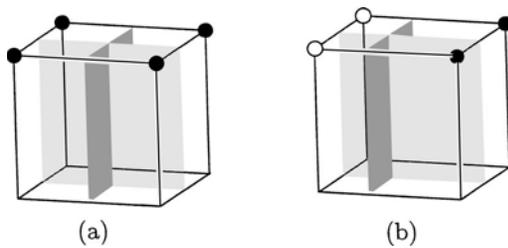
FIG. 1. Illustration of two different symmetries for a twin structure produced in a rhombohedral ferroelectric phase transition. (a) The four domains have identical size so that the system has $4mm$ symmetry. (b) Two domains are larger than the others.

systems which can result from transitions in a cubic $Pm\bar{3}m$ perovskite structure. The analysis will be performed for both equal and non-equal volume fractions of different domains in the structure. The volume fraction deviation from equal partition will cause the mesoscopic symmetry to become lower. In fact, as analyzed previously for the PMN–PT and PZN–PT systems, the effective macroscopic symmetry produced by the microscopically rhombohedral crystal structure can range from cubic $m\bar{3}m$, tetragonal $4mm$, orthorhombic $mm2$, monoclinic $m$, all the way down to triclinic $1$.[5,6] The symmetry of the multi-domain structure does not necessarily have to be a subgroup of the microscopic crystal symmetry, as shown in Fig. 1. In case (a) all four domains are identical in size. The solid circles represent the endpoints of the polarization direction vector in each domain, originating from the center of the cube. The system has two mirror planes and one four-fold rotation axis; therefore, the effective symmetry of the structure is $4mm$. In Fig. 1(b), the two right domains have equal volume fractions (represented by solid circles) and the two left domains have equal volume fraction (represented by the open circles) but the two left domains have different volume fractions from the right domains. Therefore, there is only one mirror plane in the structure and the symmetry of this twin is reduced to monoclinic $m$. (In this article if the domains have the same volume fraction they are represented by the same symbol, e.g., solid circle, open circle, solid triangle, etc., might be used, but different symbols imply different volume fractions.)

The mesoscopic symmetry analysis must distinguish the following two different situations. The first kind of domain structure analysis is on domain geometry and includes the consideration of the geometrical nature of domain configuration in space, twinning patterns as well as domain wall orientation, and positioning. The second kind of domain analysis, domain averaging, considers an average of these domains without consideration of spatial occupation details. The symmetry operations therefore refer to the global average in terms of volume fractions and the operation may not exactly bring the local structure back to itself. This article is focused on the second kind of domain structure analysis.

Of course, the domain pattern symmetry will be different if the microscopic symmetry of the crystal structure is altered. The ultimate objective is to systematically obtain all allowed "domain sets," their mesoscopic symmetry, information about the role of domain fractions in determining that symmetry, and the corresponding physical tensor properties for that domain set. Since the domain patterns can vary greatly, and since the questions of variety and resulting symmetries are not directly determined from the crystal symmetry, these possibilities can become complicated and difficult to obtain systematically. In the following we describe allowed mesoscopic symmetries in crystals having a $\Gamma$ point soft mode, which upon softening produces a proper ferroelectric phase transition. The three cases we consider correspond to polarization $(p_x, p_y, p_z)$ oriented along [100], [110], and [111], resulting in the single domain state symmetries $P4mm$, $Amm2$, and $R3m$, respectively. For the [111] polarization direction the PZM–PT and PMN–PT crystals are examples of interest. The well known $BaTiO_3$ is an example of a structural change with polarization along the [100] direction. $KNbO_3$ is an example of a material which undergoes a transition due to the spontaneous polarization toward the cube edges $\langle 110 \rangle$.

Multidomain symmmetries have been considered by Fousek et al.[7] and Fuksa and Janovec.[8] In the work of Fousek et al.[7] all volume fractions were assumed equal and thus the number of symmetries for the domain configuration were restricted. They considered multidomain symmetries for the transition from $m\bar{3}m$ to $R3m$. This corresponds to our [111] polarization ordering. The equal volume restriction was relaxed in the work of Fuksa and Janovec[8] and they listed possible symmetries for the [111] ordering. Here we consider the case of nonequal volume fractions and briefly describe an algorithm to systematically obtain all possible domain configurations. The algorithm has been implemented on computer and thus can easily yield similar results for multidomain configurations resulting from any phase transition. As examples of our procedure we list results for the experimentally interesting perovskites mentioned above of ordering along [100], [110], and [111]. We compare our results for the [111] ordering with previously published work.

## II. ALLOWED MESOSCOPIC SYMMETRIES

At the transition the symmetry reduces from the parent group symmetry $G$ to a phase of symmetry $F_1 \subset G$, which is the symmetry of the domain state $S_1$. There is a one to one correspondence between the domain states and the left cosets of $F_1$ in $G$. The group $G$ is the union of all these left cosets

$$G = F_1 + g_2 F_1 + \ldots + g_\nu F_1.$$

Each coset representative $g_i$ of $F_1$ in $G$ acting on the state $S_1$ takes it into the corresponding state $S_i$ whose symmetry is $g_i F_1 g_i^{-1}$. The set of these $\nu$ domain states formed by the transition is represented as $\mathbf{S} = \{S_1, S_2 \ldots\}$. The action of the parent group $G$ on the set $\mathbf{S}$ is a mapping of $\mathbf{S}$ to $\mathbf{S}$ which, for each element $g \in G$, assigns a state $S_b$ to a state $S_a$ for all states in $\mathbf{S}$. This mapping must be an isomorphism which is associative. The identity element of this mapping is the identity element of $G$. The action of $g$ on $\mathbf{S}$ results in a permutation of the elements in $\mathbf{S}$ and can be mapped onto a permutation matrix $D(g)$. The mapping of all operators $g \in G$ onto

permutation matrices results in a permutation representation of $G$ on $\mathbf{S}$ which contains a finite number of distinct matrices forming a permutation group $P$.

If $H$ is an arbitrary subgroup of $G$ then the $H$ orbit of the state $S_a$ is the set $\mathbf{S}_a$ of distinct states generated by applying all elements of $H$ to $S_a$. For any $H \subset G$, the set $\mathbf{S} = \{S_1, S_2 \ldots\}$ is either a single $H$ orbit $\mathbf{S} = \mathbf{S}_a$ or the union of disjoint $H$ orbits. An operation $g \in G$ takes an $H$ orbit of $S_a$ into a $gHg^{-1}$ orbit of $gS_a$. Thus the division of $\mathbf{S} = \{S_1, \ldots\}$ into $H$ orbits $\mathbf{S} = \mathbf{S}_a \cup \mathbf{S}_b \cup \ldots$ is transformed into a division of $gHg^{-1}$ orbits $\mathbf{S} = g\mathbf{S}_a g^{-1} \cup g\mathbf{S}_b g^{-1} \cup \ldots$. We will say that the two divisions of $\mathbf{S}$ under any two subgroups $H_1$ and $H_2$ of $G$, are equivalent if there exists an operation $g \in G$ which takes every orbit of $H_1$ into an orbit of $H_2$.

A multidomain crystal has an average symmetry $H$ if the effective property tensor $\overline{U}$ is invariant under the group $H$. Any effective property tensor $\overline{U}$ can be written as a function of tensor properties $U_1, U_2, \ldots U_n$ of the domain states $S_1$, $S_2, \ldots S_n$ respectively, weighted by their volume fractions. The essential information needed in order to obtain a macroscopic symmetry and thus the macroscopic properties is the knowledge of the multidomain structure, their respective volume fractions, and the maximal set of symmetries which preserve these volume fractions. The average symmetry will be determined only by the symmetry of the domains as they transform into one another under the restriction that the symmetry transformation cannot disturb the relative weighting of the domains according to the volume fraction. With this philosophy in mind, the domains which are present in the structure, with their respective group symmetries, can be interpreted as coexisting in space and being permuted by the elements of the symmetry operation corresponding to the coset decomposition. In fact, the same philosophy has been used in all ceramics and alloys when they are assumed homogeneous and isotropic. Our algorithm is based upon coset permutations corresponding to a given transition and their resulting symmetries.

We will call a domain set "connected" with respect to a group $H \subset G$, if the action of $H$ on any one of the domain states yields the entire set of domain states, the set consists of a single $H$ orbit. If $H$ is the symmetry of a multidomain structure, all elements of an $H$-connected set must have equal volume fractions. A nonconnected (NC) set of domains consists of distinct connected components. In the NC set different components do not have the same volume fraction but the domain states in each component do. The symmetry of the NC set is the intersection of the symmetries of its distinct connected components.

A multidomain structure can be represented by a vector $\mathbf{S}$ where the components represent the relative fraction of the total volume each domain occupies in the crystal. For example, a crystal composed of two domains, $S_1$ and $S_2$ of equal amounts is represented by $\mathbf{S} = (a,a,0,0,\ldots,0)$ whereas a crystal composed of the two domains in unequal amounts (necessarily nonconnected) is represented by $\mathbf{S} = (a,b,0,0,\ldots,0)$ where $a \neq b$. The symmetry $L$ of a multidomain structure consists of all operators which leave $\mathbf{S}$ invariant, i.e., all $g$ for which $D(g)\mathbf{S} = \mathbf{S}$. In the examples above, the symmetry of $\mathbf{S} = (a,a,0,0,\ldots,0)$ could include operators that interchange domains $S_1$ and $S_2$ whereas the symmetry of the nonconnected multidomain set $\mathbf{S} = (a,b,0,0,\ldots,0)$ would not.

The above procedure is also applicable in the reverse direction. This is the basis of our algorithmic approach. A more detailed discussion of the computer implementation will be given elsewhere. Here we want to emphasize the results which will be of interest for mesoscopic symmetries and tensor properties. Given a group symmetry $L$, the most general form of $\mathbf{S}$ which satisfies the matrix equation $D(g)\mathbf{S} = \mathbf{S}$ for every $g$ in $L$ gives us the most general multidomain structure with that symmetry. This procedure reduces to solving a set of simultaneous equations by computer, a matrix equation resulting for each element $g$ in $L$. The symmetry $L$ of every multidomain structure corresponds to (maps onto) one of the subgroups of $P$. Since $P$ is finite, it has a finite number of subgroups. If we consider every possible symmetry that might be allowed by a multidomain structure (corresponding to all subgroups of the permutation group $P$), and obtain the multidomain structure for each symmetry, we can obtain all possible multidomain structures. We construct by computer all subgroups of $P$ by requiring element multiplication and group closure. We start with groups of order two, check for equivalences, then go to groups of order three, etc., on up to the order of the group $P$. We then need only consider each of these subgroups, one at a time, and obtain the general domain set structure $\mathbf{S}$ for each one.

The process of starting from symmetries $L_i$ and obtaining the domain configuration needs some clarification. First there are subgroups of the permutation group $P$, defining the symmetries $L_i$, which generate the same multidomain structure as a higher symmetry group $L$. We are only interested in the complete symmetry of a structure, so in the results presented here we list only the maximal symmetry group for a given multidomain structure. Second, a multidomain structure may be equivalent to another in that it is just a rotation of the latter by a lost parent-group element. We can systematically check for equivalence for each domain structure. We list only one representative in an equivalence class. Third, suppose the symmetry $L$ determines a nonconnected vector $\mathbf{S} = (a,a,b,c,d,e)$ as a general multidomain structure of symmetry $L$. It is possible that the vector $\mathbf{S} = (0,0,b,0,d,0)$ also determines the same symmetry. This symmetry is not obtainable by omitting $b$ or $d$ (i.e., the symmetry increases when $b$ or $d$ is omitted) and the addition of the other domains (corresponding to $a$, $c$, and $e$) does not decrease the symmetry. We note that $\mathbf{S} = (0,0,b,0,d,0)$ is then a minimal domain set for the symmetry $L$ while $\mathbf{S} = (a,a,b,c,d,e)$ is not minimal. In the listing of our tables we only include the minimal domain set that determines the maximal symmetry group of the domain structure. Additional nonconnected sets which yield the same symmetry will not be listed. This allows us to present a more compact listing in the tables. In our example the vector $\mathbf{S} = (0,0,b,0,d,0)$ would yield a domain set which would be listed in our tables with symmetry $L$, because it is a minimal multidomain set. However, the vector $\mathbf{S} = (a,a,b,c,d,e)$ and its symmetry would not be listed because it yields the same symmetry, even though it is a nonconnected domain set of symmetry $L$. (See the discussion of
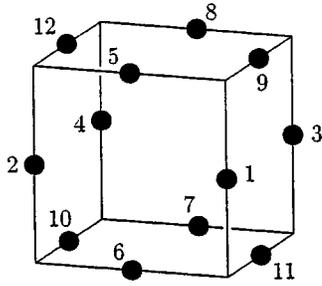
FIG. 2. Directions of polarization of domain states with orthorhombic ordering along [110].

TABLE I. All possible symmetrically distinct connected sets for ferroelectric ordering along [110]. Only nonzero contributions of the order parameters are shown in columns 3, 4, 5.

| Set | Group | $\Gamma_4^-$ | $\Gamma_3^+$ | $\Gamma_5^+$ |
|---|---|---|---|---|
| (1,2,...11,12) | $m\bar{3}m$ | $\cdots$ | $\cdots$ | $\cdots$ |
| (1,4,5,7,9,10) | $\underline{3}_{xyz}m_{\overline{xy}}$ | $\cdots$ | $\cdots$ | $(a,a,a)$ |
| (2,3,6,8,11,12) | $3_{xyz}m_{\overline{xy}}$ | $\cdots$ | $\cdots$ | $(a,a,a)$ |
| (1,5,9) | $3_{xyz}m_{\overline{xy}}$ | $(a,a,a)$ | $\cdots$ | $(a,a,a)$ |
| (2,8,11) | $3_{xyz}2_{\overline{xy}}$ | $\cdots$ | $\cdots$ | $(a,a,a)$ |
| (1,2,3,4) | $4_z/m_x m_{xy} m_z$ | $\cdots$ | $(a,0)$ | $\cdots$ |
| (5,6,7,8,9,10,11,12) | $4_z/m_x m_{xy} m_z$ | $\cdots$ | $(a,0)$ | $\cdots$ |
| (5,8,10,11) | $\bar{4}_z m_x 2_{xy}$ | $\cdots$ | $(a,0)$ | $\cdots$ |
| (5,8,9,12) | $4_z m_x m_{xy}$ | $(0,0,a)$ | $(a,0)$ | $\cdots$ |
| (1,4) | $m_{\overline{xy}} m_{xy} m_z$ | $\cdots$ | $(a,0)$ | $(a,0,0)$ |
| (1,3,6,7) | $m_{yz} m_x 2_{\overline{yz}}$ | $(0,a,-a)$ | $(a,\sqrt{3}a)$ | $(0,a,0)$ |
| (11) | $m_{yz} m_x 2_{\overline{yz}}$ | $(0,a,-a)$ | $(a,\sqrt{3}a)$ | $(0,a,0)$ |
| (1,3) | $m_z m_x 2_y$ | $(0,a,0)$ | $(a,0)$ | $\cdots$ |
| (5,7,9,10) | $2_{\overline{yz}}/m_{\overline{yz}}$ | $\cdots$ | $(a,0)$ | $(0,a,a)$ |
| (5,9) | $m_{\overline{yz}}$ | $(a,a,a)$ | $(a,0)$ | $(0,a,a)$ |
| (5,10) | $2_{\overline{yz}}$ | $(a,-a,0)$ | $(a,0)$ | $(0,a,a)$ |

a specific example in Sec. III.) Similarly, suppose a connected set $\mathbf{S}=(0,0,a,a,0,0)$ with symmetry $L$ is listed in our tables. If the addition of domains 2 and 6, corresponding to the vector $\mathbf{S}=(0,b,a,a,0,b)$, does not decrease the symmetry, this nonconnected set is not listed because it is not a minimal set yielding the symmetry $L$. (See the specific example in Sec. III.)

Thus in the listing of our results we will list: (1) the maximal symmetry for a multidomain structure; (2) only one representative for each equivalence class; and (3) only the minimal domain set determining the symmetry. We do provide the most general domain structure for each symmetry. This allows one to infer domain structures from the minimal form up to the most general form for each symmetry of an equivalence class. We check by computer each disjoint orbit to obtain the minimal domain configuration.

## III. [110] DIPOLE ORDERING IN PEROVSKITE BASED FERROELECTRIC SYSTEMS

As an example of our procedure, consider the case where the dipole moment orders at the transition toward the cube edges {110} e.g., KNbO$_3$. This ferroelectric distortion arises from the $\Gamma_4^-$ representation and changes the symmetry from that of the parent $Pm\bar{3}m$ to that of the microscopic orthorhombic crystal structure $Amm2$. There are 12 possible domain states, each being symmetrically related to the [110] domain. Those 12 domain states are the following: $1(a,a,0)$, $2(a,-a,0)$, $3(-a,a,0)$, $4(-a,-a,0)$, $5(a,0,a)$, $6(a,0,-a)$, $7(-a,0,-a)$, $8(-a,0,a)$, $9(0,a,a)$, $10(0,-a,-a)$, $11(0,a,-a)$, and $12(0,-a,a)$. Here we give the domain number and the direction of the dipole moment. The twelve domain states are represented in Fig. 2. All possible connected sets obtained by our algorithm are shown in Table I. In column 2 of Table I the point group symmetry of the mesoscopic average structure (the multidomain structure) is given. Under the symmetry transformations of the point group listed in column 2 any domain state in the set will transform into all of the listed domain states. As mentioned earlier, a set of domains is equivalent to another set if there exists a symmetry element of the parent phase which simultaneously transforms the first domain set into the second. Only one representative of each symmetry class of domains is given in column 1. For example, there are many domain sets of order 6. The domain class represented by (1,4,5,7,9,10) is connected. There is also another class, inequivalent to (1,4,5,7,9,10), consisting of 6 domains which is connected and the representative of that

class is (2,3,6,8,11,12). Only two domain classes of order 6 are connected. All other connected domain structures containing six domains are equivalent to one of these two class representatives. (Using our computer algorithm we can easily obtain a listing of all domain structures equivalent to a selected one. We do not give the complete listing of equivalent domains here because of space considerations.) In columns 3, 4, 5 we give the directions of the order parameters (OPs) for this structure. At the onset of the polarization (the primary OP) there will be coupling to secondary OPs which then become nonzero as a result of the transition. The secondary OPs of interest to us in this discussion are the components of strain. For the phase transitions from $Pm\bar{3}m$ the strain contributions are $\Gamma_1^+=(\epsilon_{xx}+\epsilon_{yy}+\epsilon_{zz})$ (volumetric strain), $\Gamma_3^+=(\epsilon_{xx}+\epsilon_{yy}-2\epsilon_{zz},\sqrt{3}\epsilon_{xx}-\sqrt{3}\epsilon_{yy})$ (deviatoric strain), and $\Gamma_5^+=(\epsilon_{xy},\epsilon_{yz},\epsilon_{xz})$ (shear strain). The OP values of the symmetric domain set are the volume-fraction-weighted average of the polarizations and strains for the structure. Along with the primary OP of dipole moment given in column 3, we give the direction of the secondary strains in columns 4 and 5, which are also connected with the mesoscopic structural symmetry.

For some domain set entries there is no dipole moment contribution, e.g., domain set (5,7,9,10) has no mesoscopic polarization (no entry for $\Gamma_4^-$) but this connected set does possess deviatoric and shear strain (entries for $\Gamma_3^+$ and $\Gamma_5^+$).

Poling fields may be applied in a hierarchal fashion to move down the chain of symmetries. For example, from the domain set (1,2...11,12), with all domains present and of equal prominence (yielding the symmetry $m\bar{3}m$), a shear stress of the form $(a,a,a)$ induces the domain set (1,4,5,7,9,10) (of symmetry $3m$) and then by imposing an electric field of the form $(a,a,a)$ the domain set (1,5,9) is obtained with symmetry $3m$.

A selection of the values for the OPs $\Gamma_4^-$, $\Gamma_3^+$, $\Gamma_5^+$ does not necessarily guarantee a unique symmetry. Notice that a strain of the form $\Gamma_5^+=(a,a,a)$ corresponds to two different symmetries with two different domain sets,

TABLE II. All possible distinct symmetries of nonconnected sets for ferroelectric ordering along [110] are given. Only nonzero contributions of the order parameters are shown in columns 3, 4, 5.

| Set | Group | $\Gamma_4^-$ | $\Gamma_3^+$ | $\Gamma_5^+$ |
|---|---|---|---|---|
| (1,2,3,4),(5,6,7,8) | $m_x m_y m_z$ | $\cdots$ | $(a,b)$ | $\cdots$ |
| (1,4),(5,8,10,11) | $2_{\overline{xy}} 2_{xy} 2_z$ | $\cdots$ | $(a,0)$ | $(a,0,0)$ |
| (1,2,3,4),(9,10) | $2_x/m_x$ | $\cdots$ | $(a,b)$ | $(0,a,0)$ |
| (1,4),(5,8,9,12) | $m_{\overline{xy}} m_{xy} 2_z$ | $(0,0,a)$ | $(a,0)$ | $(a,0,0)$ |
| (1,5,9),(2,8,11) | $3_{xyz}$ | $(a,a,a)$ | $\cdots$ | $(a,a,a)$ |
| (1,2),(9,10) | $2_{\underline{x}}$ | $(a,0,0)$ | $(a,b)$ | $(0,a,0)$ |
| (1,4),(5,7) | $1$ | $\cdots$ | $(a,b)$ | $(a,b,c)$ |
| (1,3),(5,8) | $m_x$ | $(0,a,b)$ | $(a,b)$ | $(0,a,0)$ |
| (1,3),(9) | $m_x$ | $(0,a,b)$ | $(a,b)$ | $(0,a,0)$ |
| (1,3),(10) | $m_x$ | $(0,a,b)$ | $(a,b)$ | $(0,a,0)$ |
| (9),(11) | $m_x$ | $(0,a,b)$ | $(a,b)$ | $(0,a,0)$ |
| (1),(5) | $1$ | $(a,b,c)$ | $(a,b)$ | $(a,b,c)$ |
| (1),(7) | $1$ | $(a,b,c)$ | $(a,b)$ | $(a,b,c)$ |

$\overline{3}m$ (1,4,5,7,9,10) and 32 (2,8,11), respectively. The point group symmetry $\overline{3}m$ is completely specified by $\Gamma_5^+ = (a,a,a)$ while 32 needs the additional $\Gamma_1^-$, $\Gamma_5^-$ distortions to obtain this structure. These additional distortions are not being considered in our limited discussion here, so these two domain structures cannot be separated using stress and electric field alone. Other examples of this type are evident in our tables.

In Table II all possible distinct symmetries of minimal nonconnected sets for ferroelectric ordering along [110] are given. Nonzero contributions of the order parameters are shown in columns 3, 4, 5. The list is exhaustive as far as allowed symmetries of minimal nonconnected sets are concerned and gives a representative for each class. It is not exhaustive in showing all nonequivalent nonconnected domain sets which can give the same symmetry. For example,

TABLE III. The most general domain structure for given symmetry of [110] ordering.

| Set No. | Domain set | Symmetry |
|---|---|---|
| 1 | $(a,a,a,a,a,a,a,a,a,a,a,a)$ | $m\overline{3}m$ |
| 2 | $(a,a,a,a,b,b,b,b,b,b,b,b)$ | $4_x/m_y m_z m_x$ |
| 3 | $(a,b,b,a,a,b,a,b,a,a,b,b)$ | $\overline{3}_{xyz} m_{\overline{xy}}$ |
| 4 | $(a,a,a,a,b,b,b,b,c,c,c,c)$ | $m_x m_y m_z$ |
| 5 | $(a,b,b,a,c,c,c,c,c,c,c,c)$ | $m_{\overline{xy}} m_{xy} m_z$ |
| 6 | $(a,a,a,a,b,c,c,b,c,b,b,c)$ | $4_z m_x 2_{xy}$ |
| 7 | $(a,a,a,a,b,c,c,b,c,b,c,b)$ | $4_z m_x m_{xy}$ |
| 8 | $(a,b,c,a,a,c,a,b,a,a,b,c)$ | $3_{xyz} 2_{\overline{xy}}$ |
| 9 | $(a,b,b,c,a,b,c,b,a,c,b,b)$ | $3_{xyz} m_{\overline{xy}}$ |
| 10 | $(a,b,b,a,c,d,d,c,d,c,c,d)$ | $2_{\overline{xy}} 2_{xy} 2_z$ |
| 11 | $(a,a,a,a,b,b,b,b,c,c,d,d)$ | $2_x/m_x$ |
| 12 | $(a,b,b,a,c,d,c,d,c,c,d,d)$ | $2_{\overline{xy}}/m_{\overline{xy}}$ |
| 13 | $(a,b,a,b,c,c,c,c,d,e,d,e)$ | $m_z m_x 2_y$ |
| 14 | $(a,b,a,b,b,a,a,b,c,c,d,e)$ | $m_x m_{yz} 2_{\overline{yz}}$ |
| 15 | $(a,b,b,a,c,d,d,c,c,d,d,c)$ | $m_{xy} m_{\overline{xy}} 2_z$ |
| 16 | $(a,b,c,d,a,c,d,b,a,d,b,c)$ | $3_{xyz}$ |
| 17 | $(a,a,b,c,c,d,d,e,e,f,f)$ | $2_x$ |
| 18 | $(a,b,c,a,d,e,f,g,f,d,g,e)$ | $2_{\overline{xy}}$ |
| 19 | $(a,b,b,a,c,d,c,d,e,e,f,f)$ | $1$ |
| 20 | $(a,b,a,b,c,d,d,c,e,f,g,h)$ | $m_x$ |
| 21 | $(a,b,b,c,d,e,f,g,d,f,e,g)$ | $m_{\overline{xy}}$ |
| 22 | $(a,b,c,d,e,f,g,h,i,j,k,l)$ | $1$ |

the nonconnected domain set (1,2,3,4),(5,6,7,8) yields the symmetry $m_x m_y m_z$. However, the non-connected domain set (1,2,3,4),(5,6,7,8),(9,10,11,12) also yields the same symmetry. Only minimal non-connected sets, representatives of each symmetry, are listed. Also, an allowed nonconnected set may not be shown because the symmetry (or the equivalent symmetry) it determines can be obtained from a connected set of domains. For example, the connected domain set (1,3) yields the symmetry $m_z m_x 2_y$. The domain set $(a,b,a,b,0,0,0,0,0,0,0,0)$ is nonconnected but it determines the same symmetry as that of $(a,0,a,0,0,0,0,0,0,0,0,0)$, a connected set. The nonconnected domain set $(a,b,a,b,0,0,0,0,0,0,0,0)$ is not listed in Table II.

In Table III we list the most general domain structure allowed by the representative symmetry of a given class. This allows the reader to obtain a set of domain structures yielding the same symmetry, progressing from the minimal domain structure to the more general. The discussion of the two examples in the paragraph above can be developed by considering the sets of numbers 4 and 13, respectively, of Table III.

For a structure composed of domains 1 and 3, with equal volume fractions, the domain set is connected and the symmetry is $m_z m_x 2_y$ (see Table I). If a shear stress, corresponding to $\Gamma_5^+(\pm a,0,0)$, is added, then the domains are of different energies, their volume fractions are no longer equal, the domain set is not connected but consists of two components (1) and (3) respectively, and the symmetry changes to $m_z$. [This domain structure is equivalent to the domain structure (9),(11) of Table II.] There is an also an associated change in dipole moment direction.

## IV. [100] DIPOLE ORDERING IN PEROVSKITE BASED FERROELECTRIC SYSTEMS

Now consider the case where the dipole moment orders at the transition along the {100} cubic directions, e.g. $BaTiO_3$. This ferroelectric distortion also arises from the $\Gamma_4^-$ representation and changes the symmetry of the microscopic crystal structure from $Pm\overline{3}m$ to the tetragonal $P4mm$ structure. There are six possible domain states with each being symmetrically related to the [100] domain. The six domain states are represented in Fig. 3. The labeling of OP directions are the following: $1(a,0,0)$, $2(-a,0,0)$, $3(0,0,a)$, $4(0,0,-a)$, $5(0,a,0)$, $6(0,-a,0)$. All possible connected sets arising from this transition are given in Table IV. In Table V all possible distinct symmetries of nonconnected sets for ferroelectric ordering along [100] are given. Table VI lists the most general domain structure allowed by the symmetry representing each equivalence class for the [100] ordering.

As an example of the use of the symmetry tables for ordering along [100] consider the case discussed by Erhart and Cao.[5,6] As can be seen from Table IV, when a poling field is applied along [111] rather than one of the polarization directions it leads to a three domain state containing the domain set (1,3,5). If only two of these domains remain due to additional poling then only the symmetry $mm2$ is possible. This follows from the fact that domain sets (1,3) and (1,5) are in the class corresponding to entry (3,6) in Table IV. If

J. Appl. Phys., Vol. 94, No. 8, 15 October 2003

Hatch, Stokes, and Cao      5225
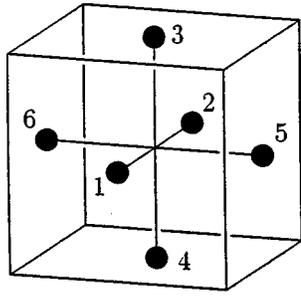


FIG. 3. Directions of polarization of domain states with tetragonal ordering along [100].

TABLE V. All possible distinct symmetries of nonconnected sets for ferroelectric ordering along [100] are given. Only nonzero contributions of the order parameters are shown in columns 3, 4, 5.

| Set | Group | $\Gamma_4^-$ | $\Gamma_3^+$ | $\Gamma_5^+$ |
|---|---|---|---|---|
| (1,2),(3,4) | $m_x m_y m_z$ | $\cdots$ | $(a,b)$ | $\cdots$ |
| (1,2),(5) | $m_x m_z 2_y$ | $(0,0,a)$ | $(a,b)$ | $\cdots$ |
| (3),(5) | $m_x$ | $(0,a,b)$ | $(a,b)$ | $(0,a,0)$ |
| (1,5),(3) | $m_{\overline{xy}}$ | $(a,a,b)$ | $(a,0)$ | $(a,b,b)$ |
| (1),(3),(5) | 1 | $(a,b,c)$ | $(a,b)$ | $(a,b,c)$ |

the domains are of different volume fractions then Tables V and VI indicate the symmetry is reduced to $m$.

## V. [111] DIPOLE ORDERING IN PEROVSKITE BASED FERROELECTRIC SYSTEMS

Now consider the case where the dipole moment orders at the transition along the [111] cube diagonals, e.g., PZN–PT. This ferroelectric distortion also arises from the $\Gamma_4^-$ representation and changes the symmetry of the microscopic crystal structure from $Pm\overline{3}m$ to $R3m$. There are eight possible homogeneous domain states with each being symmetrically related to the [111] domain. The eight domain states are represented in Fig. 4. The labeling of OP directions are: $1(a,a,a)$, $2(a,-a,-a)$, $3(-a,a,-a)$, $4(-a,-a,a)$, $5(-a,-a,-a)$, $6(-a,a,a)$, $7(a,-a,a)$, $8(a,a,-a)$. All possible connected sets arising from this transition are shown in Table VII. In Table VIII all possible distinct symmetries of nonconnected sets for ferroelectric ordering along [111] are given. Table IX lists the most general domain structure allowed by the symmetry representing the equivalence class for the [111] ordering.

Although this case was investigated by Fousek *et al.*[7] we found some differences. The set [135] of Fousek *et al.*[7] corresponds to our labeling of domains (1,4,5). The domain set (1,4,5) does not show up in our listing of connected sets in Table VII and it is not equivalent (not just a "rotated" version) to the three domain set (2,3,4) which does appear in that table. The symmetry of domain set (1,4,5) is $m_{\overline{xy}}$ according to Fousek *et al.*[7] They considered only equal volume fractions to get this symmetry. However, the $m_{\overline{xy}}$ symmetry is obtained in our work by the minimal domain set (1)(4), shown in Table VIII. Moreover, by adding the third domain to obtain the domain set (1)(4)(5), which is not a minimal

nonconnected domain set for this symmetry, we do not diminish the symmetry from $m_{\overline{xy}}$. None of the three volume fractions need to be equal to obtain this symmetry. Thus our expanded consideration to nonconnected sets provides a broader understanding of possible three-domain configurations yielding the $m_{\overline{xy}}$ symmetry.

Similarly, [1235] (this domain set corresponds to our labeling (1,2,4,5)) yields the symmetry $m_{\overline{xz}}$ according to Fousek *et al.*[7] The same symmetry is obtained by the nonconnected, nonminimal domain set (1,4)(2)(5) or the nonconnected minimal domain set (1,4)(2). This domain set is equivalent to our entry (1)(2,3) in Table VIII.

The domain set [1238] corresponds to our labeling (1,2,4,7). This domain set yields the symmetry $3_{xy\overline{z}}m_{\overline{xz}}$ according to Fousek *et al.*[7] The minimal connected domain set (1,2,4) yields this symmetry and is equivalent to our entry (2,3,4) in Table VII. The nonminimal, nonconnected set (1,2,4)(7) does not destroy any symmetry and thus yields the same symmetry $3_{xy\overline{z}}m_{\overline{xz}}$.

As we compare our results of [111] ordering with those of Fuksa and Janovec[8] we see that there are some differences in presentation of results. We distinguish inequivalent domain structures in our listings where they do not. Fuksa and Janovec list many nonconnected sets which are not minimal. To systematically obtain non-connected sets which are not minimal we give the most general domain structure for a given symmetry so that the nonminimal domain sets can be constructed. However, their results and ours generally agree.

An example of field induced domain reorientation was recently described by Chen *et al.*[9] The domains corresponded to dipole moment ordering along ⟨111⟩. Thus there

TABLE VI. The most general domain structure for given symmetry of [100] ordering.

| Set No. | Domain set | Symmetry |
|---|---|---|
| 1 | $(a,a,a,a,a,a)$ | $m\overline{3}m$ |
| 2 | $(a,a,b,b,a,a)$ | $4_z/m_x m_{xy} m_z$ |
| 3 | $(a,a,b,b,c,c)$ | $m_x m_y m_z$ |
| 4 | $(a,a,b,c,a,a)$ | $4_z/m_x m_{xy} m_z$ |
| 5 | $(a,b,a,b,a,b)$ | $3_{xyz}m_{\overline{xy}}$ |
| 6 | $(a,a,b,b,c,d)$ | $m_x m_z 2_y$ |
| 7 | $(a,a,b,c,c,b)$ | $m_{yz} m_x 2_{\overline{yz}}$ |
| 8 | $(a,b,c,c,d,d)$ | $2_x$ |
| 9 | $(a,b,c,c,b,a)$ | $2_{\overline{xy}}$ |
| 10 | $(a,a,b,c,d,e)$ | $m_x$ |
| 11 | $(a,b,c,d,a,b)$ | $m_{\overline{xy}}$ |
| 12 | $(a,b,c,d,e,f)$ | 1 |

TABLE IV. All possible symmetrically distinct connected sets for ferroelectric ordering along [100]. Only nonzero contributions of the order parameters are shown in columns 3, 4, 5.

| Set | Group | $\Gamma_4^-$ | $\Gamma_3^+$ | $\Gamma_5^+$ |
|---|---|---|---|---|
| (1,2,3,4,5,6) | $m\overline{3}m$ | $\cdots$ | $\cdots$ | $\cdots$ |
| (1,2,5,6) | $4_z/m_x m_{xy} m_z$ | $\cdots$ | $(a,0)$ | $\cdots$ |
| (3,4) | $4_z/m_x m_{xy} m_z$ | $\cdots$ | $(a,0)$ | $\cdots$ |
| (1,3,5) | $3_{xyz}m_{\overline{xy}}$ | $(a,a,a)$ | $\cdots$ | $(a,a,a)$ |
| (3) | $4_z m_x m_{xy}$ | $(0,0,a)$ | $(a,0)$ | $\cdots$ |
| (3,6) | $m_{yz} m_x 2_{\overline{yz}}$ | $(0,a,-a)$ | $(a,\sqrt{3}a)$ | $(0,a,0)$ |
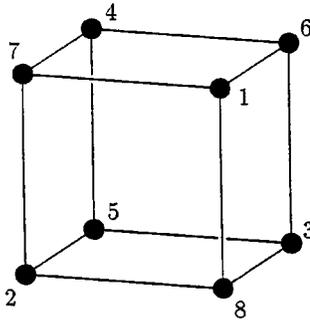
FIG. 4. Directions of polarization of domain states with rhombohedral ordering along [111].

are eight domain states, shown again in Fig. 5(a). They divided the process of polarization into four regions. In the first region only a small field was applied [see Fig. 5(b)] and thus only fairly low energy domain switching could take place, namely 180° switching which removed domains 3 and 8. Thus, with no lattice distortion the domain configuration becomes that shown in Fig. 5(b). As indicated in the figure, the electric field of direction $[0\bar{1}1]$ simultaneously selects domain set (4,7) of symmetry $m_{yz}m_x2_{\overline{yz}}$ (symmetrically equivalent to the domain set (3,8) shown in Table VII) and domain set (1,2,5,6) (symmetrically equivalent to the domain set (1,4,5,8) shown in Table VII). This latter domain set contains all symmetry elements of the first, thus yielding the nonconnected domain set $(1,2,5,6)(4,7)$ of symmetry $m_{yz}m_x2_{\overline{yz}}$. In the second region a stronger field selects domain set (4,7), resulting in two domains and the symmetry remains $m_{yz}m_x2_{\overline{yz}}$. In region three a rotation of the polarization takes place and the microscopic domain symmetry changes. Our model does not apply to this process. Due to strong-field poling the fourth region is a single domain with dipole moment aligned along $[0\bar{1}1]$ and of symmetry $m_{yz}m_x2_{\overline{yz}}$ (symmetrically equivalent to the listing of domain structure (11) in Table I).

## VI. DISCUSSION AND CONCLUSION

Domain average engineering has shown great success in producing superior piezoelectric crystals.[1–4] The effective properties and symmetries are determined by the configura-

TABLE VII. All possible symmetrically distinct connected sets for ferroelectric ordering along [111]. Only nonzero contributions of the order parameters are shown in columns 3, 4, 5.

| Set | Group | $\Gamma_4^-$ | $\Gamma_3^+$ | $\Gamma_5^+$ |
|---|---|---|---|---|
| (1,2,3,4,5,6,7,8) | $m\bar{3}m$ | $\cdots$ | $\cdots$ | $\cdots$ |
| (2,3,4,6,7,8) | $\bar{3}_{xyz}m_{\overline{xy}}$ | $\cdots$ | $\cdots$ | $(a,a,a)$ |
| (1,5) | $\bar{3}_{xyz}m_{\overline{xy}}$ | $\cdots$ | $\cdots$ | $(a,a,a)$ |
| (1,2,3,4) | $4_z3_{xyz}m_{xy}$ | $\cdots$ | $\cdots$ | $\cdots$ |
| (1,4,6,7) | $4_zm_ym_{\overline{xy}}$ | $(0,0,a)$ | $(a,0)$ | $\cdots$ |
| (1,4,5,8) | $m_{xy}m_{\overline{xy}}m_z$ | $\cdots$ | $(a,0)$ | $(a,0,0)$ |
| (2,3,4) | $3_{xyz}m_{\overline{xy}}$ | $(a,a,a)$ | $\cdots$ | $(a,a,a)$ |
| (1) | $3_{xyz}m_{\overline{xy}}$ | $(a,a,a)$ | $\cdots$ | $(a,a,a)$ |
| (1,4) | $m_{xy}m_{\overline{xy}}2_z$ | $(0,0,a)$ | $(a,0)$ | $(a,0,0)$ |
| (3,8) | $m_xm_{yz}2_{\overline{yz}}$ | $(0,a,-a)$ | $(a,\sqrt{3}a)$ | $(0,a,0)$ |

TABLE VIII. All possible distinct symmetries of nonconnected sets for ferroelectric ordering along [111] are given. Only nonzero contributions of the order parameters are shown in columns 3, 4, 5.

| Set | Group | $\Gamma_4^-$ | $\Gamma_3^+$ | $\Gamma_5^+$ |
|---|---|---|---|---|
| (1,5),(2,3,6,7) | $2_{\overline{xy}}/m_{\overline{xy}}$ | $\cdots$ | $(a,0)$ | $(a,b,b)$ |
| (1,5),(4,8) | $2_{\overline{xy}}/m_{\overline{xy}}$ | $\cdots$ | $(a,0)$ | $(a,b,b)$ |
| (1,5),(2,7) | $2_{\overline{xy}}$ | $(a,-a,0)$ | $(a,0)$ | $(a,b,b)$ |
| (1,5),(2,6),(3,7) | $1$ | $\cdots$ | $(a,b)$ | $(a,b,c)$ |
| (1,6),(3,8) | $m_x$ | $(0,a,b)$ | $(a,b)$ | $(0,a,0)$ |
| (1),(2,3) | $m_{\overline{xy}}$ | $(a,a,b)$ | $(a,0)$ | $(a,b,b)$ |
| (1),(4) | $m_{\overline{xy}}$ | $(a,a,b)$ | $(a,0)$ | $(a,b,b)$ |
| (1),(6,7) | $m_{\overline{xy}}$ | $(a,a,b)$ | $(a,0)$ | $(a,b,b)$ |
| (1),(8) | $m_{\overline{xy}}$ | $(a,a,b)$ | $(a,0)$ | $(a,b,b)$ |
| (1),(2),(3) | $1$ | $(a,b,c)$ | $(a,b)$ | $(a,b,c)$ |
| (1),(2),(7) | $1$ | $(a,b,c)$ | $(a,b)$ | $(a,b,c)$ |

tion of domains at the mesoscopic level but still intrinsically linked to the microscopic crystal symmetry. There are many different possibilities of domain structure configurations for each given crystal system. Fousek et al.[7] composed a partial list of domain averaging for a cubic–rhombohedral ferroelectric system. Fuksa and Janovec[8] then extended considerations to nonconnected sets for this same species. Our extension adds the results of the other two ferroelectric phase transition systems, i.e., cubic–tetragonal, cubic–orthorhombic, and also considers the problem with the goal of systematic implementation for other phase transitions. Since the analysis depends only on the symmetries of the parent and product phases the results obtained here are not dependent on the specific perovskite structure. This structure was used because of its practical importance in many ferroelectric materials. Our results will apply for any structure with the $m\bar{3}m$ symmetry with a dipole moment ordering corresponding to the $\Gamma_4^-$ soft mode.

ISOTROPY contains the computer implementation[10] of our algorithm and obtains domain average structures for any space group phase transition. For domain structure analysis of the first kind (domain geometry), the task is more in-

TABLE IX. The most general domain structure for given symmetry of [111] ordering.

| Set No. | Domain set | Symmetry |
|---|---|---|
| 1 | $(a,a,a,a,a,a,a,a)$ | $m\bar{3}m$ |
| 2 | $(a,a,a,a,b,b,b,b)$ | $4_z3_{xyz}m_{xy}$ |
| 3 | $(a,b,b,b,a,b,b,b)$ | $3_{xyz}m_{\overline{xy}}$ |
| 4 | $(a,b,b,a,a,b,b,a)$ | $m_{xy}m_{\overline{xy}}m_z$ |
| 5 | $(a,b,b,a,b,a,a,b)$ | $4_zm_ym_{\overline{xy}}$ |
| 6 | $(a,b,b,b,c,d,d,d)$ | $3_{xyz}m_{\overline{xy}}$ |
| 7 | $(a,a,b,b,a,a,b,b)$ | $2_x/m_x$ |
| 8 | $(a,b,b,c,a,b,b,c)$ | $2_{\overline{xy}}/m_{\overline{xy}}$ |
| 9 | $(a,b,a,b,b,a,b,a)$ | $m_xm_z2_y$ |
| 10 | $(a,a,b,c,a,a,c,b)$ | $m_xm_{yz}2_{\overline{yz}}$ |
| 11 | $(a,b,b,a,c,d,d,c)$ | $m_{xy}m_{\overline{xy}}2_z$ |
| 12 | $(a,a,b,b,c,c,d,d)$ | $2_x$ |
| 13 | $(a,b,c,d,a,c,b,d)$ | $2_{\overline{xy}}$ |
| 14 | $(a,b,c,d,a,b,c,d)$ | $1$ |
| 15 | $(a,b,c,d,b,a,d,c)$ | $m_x$ |
| 16 | $(a,b,b,c,d,e,e,f)$ | $m_{\overline{xy}}$ |
| 17 | $(a,b,c,d,e,f,g,h)$ | $1$ |
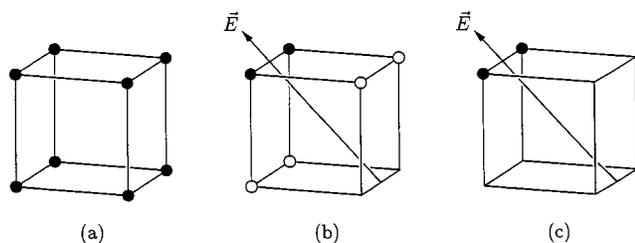
FIG. 5. Symmetry changes resulting from a $[0\bar{1}1]$ field: (a) OP directions for rhombohedral ordering; (b) nonconnected domain configuration for weak poling field; and (c) connected domain set of symmetry $m_{yz}m_x2_{\bar{yz}}$ for strong poling field.

volved and there is as yet no systematic procedure available to provide an exhaustive list of domain pattern symmetries.

The domain average symmetry considered in this paper is applicable to crystals having a large number of domains. For such a case, the domains form a kind of nanocomposite with sets of domains. Each set contains domains of equal volume and the domains have certain predetermined symmetries based on the underlying parent crystal symmetry.

We point out again that our list of symmetries include all possible ones up to equivalence. Some multidomain mesoscopic symmetries given here may be difficult to physically realize. If the domain size becomes relatively large, say beyond microns, one must consider the spatial configuration of domains and the orientation of domain walls that join these domains. The limited number of domains in each given finite sample may invalidate the statistical treatment used in this article. Such large domain cases belong to the first kind of mesoscopic symmetry problem mentioned above, which is not discussed here.[11]

## ACKNOWLEDGMENTS

[1] S. E. Park and T. R. Shrout, J. Appl. Phys. **82**, 1804 (1997).
[2] J. Kuwata, K. Uchino, and S. Nomura, Jpn. J. Appl. Phys., Part 1 **21**, 1298 (1982).
[3] J. Yin, B. Jiang, and W. Cao, IEEE Trans. Ultrason. Ferroelectr. Freq. Control **47**, 285 (2000).
[4] R. Zhang, B. Jiang, and W. Cao, J. Appl. Phys. **90**, 3471 (2001).
[5] J. Erhart and W. Cao, J. Appl. Phys. **86**, 1073 (1999).
[6] J. Erhart and W. Cao, J. Mater. Res. **16**, 570 (2001).
[7] J. Fousek, D. B. Litvin, and L. E. Cross, J. Phys.: Condens. Matter **13**, L33 (2001).
[8] J. Fuksa and V. Janovec, J. Phys.: Condens. Matter **14**, 3795 (2002).
[9] K. Chen, X. Zhang, F. Fang, and H. Luo, arXiv:cond-mat/0206473 (2002).
[10] H. T. Stokes and D. M. Hatch, ISOTROPY software and documentation is available over the internet at ⟨www.physics.byu.edu/~stokesh/isotropy.html⟩ (2002), Session 6 in the tutorial shows specifically how ISOTROPY was used to analyze multidomain symmetries discussed in this article.
[11] J. Fousek and L. E. Cross, Ferroelectrics **252**, 171 (2001).